Submodule Level Distributed Maximum Power Point Tracking PV Optimizer with Integrated Architecture

Feng Wang[†], Tianhua Zhu, Fang Zhuo, Hao Yi and Shuhuai Shi

State Key Laboratory of Electrical Insulation and Power Equipment
Xi'an Jiaotong University, Xi'an, 710049 China

Abstract

Distributed maximum power point tracking (DMPPT) concept is widely adopted in photovoltaic system to avoid mismatch loss. However, high cost and complexity hinder its further promotion in practice. Based on the concept of DMPPT, this paper presents an integrated submodule level half-bridge stack structure along with optimal current point tracking (OCPT) control algorithm. In this full power processing integrated solution, the number of power switches and passive components is greatly decreased. On the other hand, only one current sensor and related AD unit are needed to perform the ideal maximum power generation of all PV submodules in any irradiance case. The proposal can totally eliminate different small-scaled mismatch effects in real-word condition and true maximum power point of each PV submodule can be achieved and ideal maximum power output of whole PV system can be thereby achieved. Compared with current solutions, the proposal further develops the integration level of submodule DMPPT solutions with lower cost and smaller size. Moreover, the individual MPPT tracking of all submodules are guaranteed in the meanwhile.

Key words: Submodule, PV, mismatch, ideal maximum power generation

I. INTRODUCTION

Photovoltaic (PV) systems have been widely built all over the world to utilize solar energy directly. Since the ideal irradiance is practically impossible in real-world, the PV panels often suffer different shading case in daily operation. Moreover, non-uniform aging and accidental damage of PV panels frequently occur and impact adversely on the performance of PV systems, especially in the middle and late periods of their service life. Aforementioned cases can be collectively called mismatch. Due to the difficult prediction of shading cases and high cost of replacing aged (or damaged) PV units by new ones, the mismatch in PV systems significantly deteriorates the effectiveness of energy harvest, particularly in centralized and string level maximum power point tracking (MPPT) based PV systems. Moreover, the mismatch case also leads to multiple maximum power points (MPP) on the power-voltage curve of original PV array or PV string which leads to failure of most MPPT algorithms and power oscillation.[1-3]

Therefore, it is appealing to improve energy efficiency of current PV systems in mismatch cases. Distributed maximum power point tracking (DMPPT) PV systems have drawn increased attention because it decouples the PV units from adjacent ones through a dedicated MPPT converter. The module level MPPT converter, commonly referred to as "PV optimizer" or "module integrated converter (MIC)," is widely explored and it is concerned essentially with the current PV systems. Since small-scale mismatch case happens more frequently, such as in portable solar power system, the performance of current commercial PV optimizer-based solar system is still less than satisfactory in such cases. Submodule level DMPPT solution developed rapidly in recent years. Submodule level MPPT can be regarded as a further step to address the small-scale mismatch issues with better power recovery ability. The submodule DMPPT converters are designed to fit the junction box of commercial PV panel and perform MPPT at the submodule level to eradicate small scale mismatch power loss.

Although mismatch loss can be recovered through the submodule DMPPT with independent MPPT control, the implementation cost of the system will also multiply due to the increasing components. A set of power switches, passive devices (inductors and capacitors), MPPT control ICs, current

sensors, voltage sensors and corresponding AD/DA converters are needed for every PV submodule. As PV is a cost-sensitive market, the increasing components result in high weight, large size, high cost, low efficiency and low index of mean time before failure (MTBF). Above drawbacks prevent the submodule DMPPT concept from spreading and popularizing. Since the maximum power point (MPP) voltage (Vmpp) is not a strong function of the irradiance, unlike the MPP current Impp, on this way, many methods are proposed to simplify the submodule level DMPPT solutions. In paper [4], an unified input voltage control strategy is proposed which can recover nearly all power loss caused by small scaled mismatch case. In [5], a close-to-optimal distributed control approach is presented that allows autonomous submodule control without the need for a central controller or any communication among the PV submodules. Although above methods are proposed with less cost and fewer components, both of them are still quasi-MPPT solutions. In fact, with "virtual parallel" operation, the operating voltages of PV submodules are regulated to be equal while the physical series connection of the DC-DC converters is maintained to achieve enough output voltage. Papers [6, 7] utilize Gallium-Nitride device in submodule Buck converter to achieve high conversion efficiency and reduced size. Nonetheless, higher cost is still the bottleneck for large-scale enterprise application. In [8, 9], time-sharing MPPT control solutions are proposed and the true MPP of each PV submodule can be achieved. However, the number of the components of the circuit is not satisfying from the cost perspective. In [3, 10], differential power processing structure based submodule DMPPT solutions are proposed. This structure only processes partial power generated from PV unit with inherently high efficiency comparing with other full power processing methods. Nonetheless, the complexity of this MPPT algorithm makes it difficult to promote and the neighbor submodules cannot be decoupled easily from each other. It was shown in paper [11, 12] that tracking the output current can realize MPPT functionality with greatly reduced number of sensors and further simplified controller and inductor.

In this paper, an integrated half-bridge stack structure with a common LC filter is used in submodule distributed power generation system. In this full power processing structure, an optimal current point tracking (OCPT) control strategy is applied accordingly which only requires one current sensor, one AD unit and one digital controller performing submodule level maximum power tracking control. The proposal can totally eliminate small-scaled mismatch effects in real-word condition and the ideal maximum power point of each PV submodule can be achieved precisely even under irradiance change. Compared with current solutions, the proposal further develops the integration level of submodule DMPPT solutions with less components, lower cost, smaller size

and higher MTBF index. Simulation and experimental results show that the ideal MPPs of submodules can be exactly reached separately.

II. ANALYSIS OF THE PROPOSED INTEGRATED SOLUTION

A. Shading case study

For the centralized or string level MPPT PV systems, the consequences of the mismatch are degradations in total power harvest and multiple maxima power points issues on the power-voltage curve. The global maximum power point (GMPP) of the shaded PV system can be reached through some advanced algorithms. However, such a power is still lower than the ideal maximum power which is the sum of the available maximum powers of each PV units, since the shaded part of the PV system would limit the output current of the non-shaded part [13, 14]. Fig.1 shows a standard PV panel consisting of PV cells connected in series, divided into three submodules by anti-parallel bypass diodes which help
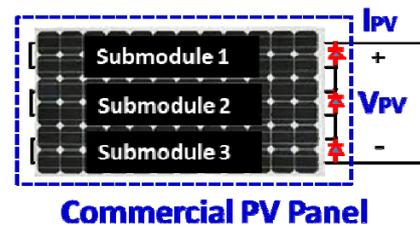

Fig.. 1. Structure of commercial PV panel.

reduce the appearance of hot spots and mitigate destructive effects in the PV submodules.

Fig.2 shows the mismatch case that submodule 3 is shaded. The output P-V curves of submodule 1 and 2 are shown as blue dotted lines. The output P-V curve of submodule 3 is shown as red dotted line. The output P-V curve of this partial shaded PV panel is depicted as red solid curve. The black
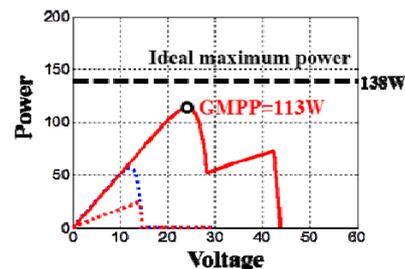

Fig.. 2. Output P-V curve of shaded PV panel.

dashed line indicates the ideal maximum power of the PV panel (138W), which is about 18% higher than the value of GMPP (113W) in this case.

Functionally, current commercial PV optimizers can only achieve the GMPP point of the red curve in Fig.2. The mismatch power loss cannot be totally recovered. The

topologies of current solutions can be classified into three categories according to their voltage gain: Buck type, Boost type and Buck-Boost type. The pros and cons have already been analyzed in detail in previous literatures [4, 15, 16].

B. Power Circuit

In this paper, synchronized Buck converter stack with a common LC filter is adopted as topology of submodule maximum power generation system for its simpler structure, fewer components and easier achievements of MPPT in series connection.

As shown in Fig.3, the input side of each buck converter is connected in parallel with a PV submodule. From the output sides, these inductor-free buck converters are connected in series to achieve higher output voltage with a common LC filter. Each half bridge is controlled by a pair of complementary duty cycle signals (eg. D_1 and $(1-D_1)$) separately. In this structure, lower power rating devices and higher voltage gain can be adopted for submodule PV application. This structure can be directly connected to DC bus or DC link of commercial micro-inverter to perform grid-tied power generation. In this structure, the single capacitor is smaller than the total combined set of capacitors if interleaving carrier is adopted, each of which is normally used with every buck DC-DC converter. The use of a single
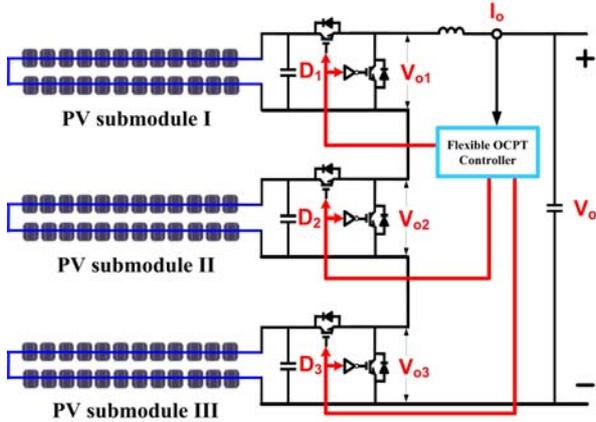

Fig. 3. Structure of power circuit.

inductor also reduces cost and weight while increasing the efficiency in extracting maximum power from the PV submodules.

In this architecture, static working principle analysis is conducted below. Under steady state conditions, the output voltage of each Buck converter and its corresponding PV submodule voltage satisfy equation (1).

$$\frac{V_{o1}}{V_{pv1}} = D_1, \frac{V_{o2}}{V_{pv2}} = D_2, \frac{V_{o3}}{V_{pv3}} = D_3, \cdot \tag{1}$$

Similarly, the total output current and each photovoltaic current satisfy equation (2).

$$I_o = \frac{I_{pv1}}{D_1} = \frac{I_{pv2}}{D_2} = \frac{I_{pv3}}{D_3} \tag{2}$$

Since the average value of voltage across the single inductor L can be considered 0 over a switching period, V_o is expressed as:

$$V_o = \sum_{i=1}^{3} V_{oi} = \sum_{i=1}^{3} V_{pvi} \cdot D_i = \sum_{i=1}^{3} V_{pvi} \cdot \frac{I_{pvi}}{I_o} \tag{3}$$

Obviously,

$$V_o \cdot I_o = \sum_{i=1}^{3} V_{pvi} \cdot I_{pvi} \tag{4}$$

From the above equations, it can be noted that regardless of mismatch conditions of PV submodules, the output power of all submodules can be obtained at the general output side. Thus, all submodules can operate at their individual MPPs and the ideal maximum output power can be extracted from the PV units.

C. Simplified OCPT control strategy

Mostly, the DC voltage (V_o) is controlled by micro-inverter which can be regarded as a controllable current sink. Since the perturbation interval of 2nd maximum power seeking process is much longer than that in submodule level converters, the V_o can be considered temporarily fixed during the perturbation of Buck converters. With a given V_o,
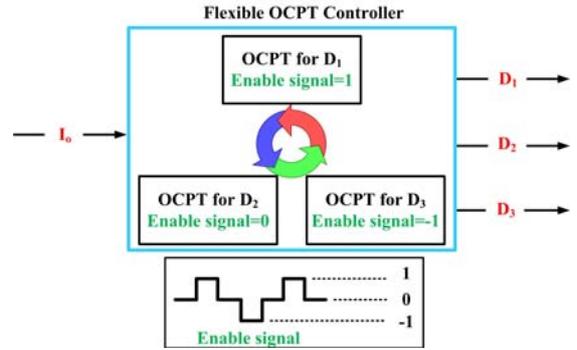
(a) Schematic of OCPT block
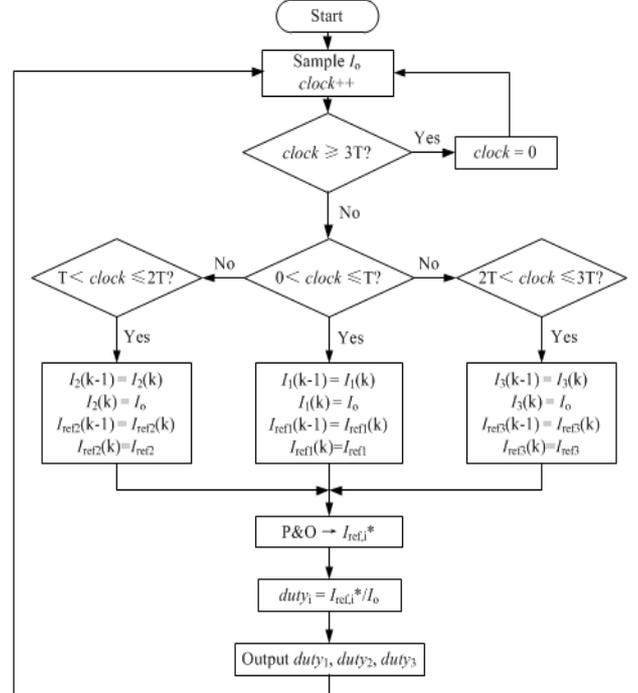
(b) Flow chart of time-sharing OCPT control
Fig. 4. The diagram of control block.

maximizing the string current (I_o) is equivalent to maximizing the total output power with a fixed V_o. Therefore, the half bridges, as shown in Fig.3, iterate frequently to maximize the total output current I_o for a given V_o, which is exactly the fundamental principle of proposed OCPT strategy.

In our proposed system, time-sharing OCPT control is adopted on the output side of the module so that only one controller is sufficient. The flow diagram of this control strategy is presented in Fig.4 (b). The parameter clock is progressively increased and its value decides which submodule is to be tracked. For example, if the value of clock is between 0 and T, it means that the controller is doing OCPT for submodule 1. Similarly, when clock is between T and 2T, submodule 2 is under OCPT. When clock exceeds 3T, it is reset to 0 and the above process repeats.

As aforementioned, the output voltage V_o in Fig.3 can be considered temporarily constant. According to equation (3) and (4), the variation of I_o can just represent the variation of the total output power P_o. Also, in [17], the single output parameter MPPT control is proved to be possible for nearly all practical load types. Consequently, a single current sensor for output current I_o is sufficient to achieve the maximum power generation control.

Fig. 5 shows the working principle of the directly duty cycle controller. The single current sensor based OCPT controller conducts seeking MPP on PV submodules in turn, which means at any time, the variation of the total output power P_o equals to the power variation of submodule being tracked. The Perturb and Observe (P&O) algorithm is adopted to impose perturbation on photovoltaic current of submodules instead of typical photovoltaic voltage. Generally, P-I curve has a similar shape to P-V curve. Hence, according to the sign of $\Delta I_o(k) \cdot \Delta I_{ref}(k)$, the current reference of next period $I_{ref}(k+1)$ can be derived. Then the objective duty ratio can be calculated as: $D(k+1) = I_{ref}(k+1)/I_o$ and a PWM signal of this duty cycle is generated by the OCPT controller to drive the relative switch and bring the photovoltaic current to
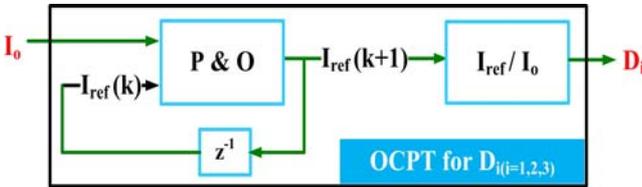

Fig. 5. Directly duty cycle controller.

the expected reference. The directly duty cycle control no longer need to detect the real-time voltage of each PV submodule and three voltage sensors are thereby saved.

III. COMPARISON WITH CURRENT SOLUTIONS

Several relative papers are compared to justify the improvement of the proposal. The comparison is given from following aspects: number of power components required in the power circuit, number of control related components in the control part and other characteristics of the integrated PV module. Before the comparison, several features need some explanation. The ideal maximum power indicates the sum of the available maximum powers of each PV units as shown in Fig.2. The output power ratio indicates the normalized ratio of actual output power to ideal maximum power. The voltage gain shows the

ration of output voltage of the integrated PV module to the voltage of PV submodule. The optimal power region means the feasible voltage (or current) region of DMPPT PV system which makes all PV units working on their individual MPPs in given irradiance cases [15].

Five latest counterparts are selected to execute the comparative analysis. Together with our proposal, six methods are studied and compared from different perspectives. We named the counterparts as following:

✧ *Control strategy I：[6, 7];*

Control strategy I introduces independent MPPT control for each PV submodule inside a standard PV panel and it regulates the duty cycle of the power stage separately in order to decouple a PV submodule from the others inside a PV panel. Gallium-Nitride device are used to achieve high conversion efficiency and reduced size. Nonetheless, higher cost is still the bottleneck for large-scale enterprise application.

✧ *Control strategy II：[4, 17, 18];*

An unified output voltage strategy with single MPPT controller is proposed as Control strategy II. In this structure:

1) A single MPPT unit is sensing the total output power of the converter system with only one pair of voltage and current sensors;

2) Three Buck MPPT converters share a common V_{ref} coming from the single MPPT unit;

3) Each Buck MPPT converter owns an independent control loop. This control method only achieves a quasi-MPPT state.

The "virtual parallel" operation is introduced so that the operating voltages of PV submodules are regulated to be equal under different mismatch cases, while the physical series connection of the dc/dc converters is maintained.

From (21), it is clear that the characteristics the PI type back-EMF estimator are the same as those of a first-order low-pass filter.

✧ *Control strategy III：[8];*

Based on Control strategy II, Control strategy III is applied in multi-panel level simplification. The unified output control is applied on each PV panel and the multiple unified controllers of four PV panels are optimized through time sharing MPPT control. In this structure, the number of MPPT IC is decreased by the time-sharing control strategy of four buck converters and related PV panels. The output voltage of buck converters and total output current are sampled as inputs for MPPT control unit. Under the control of a periodic enable signal, the MPPT unit operates P&O algorithm for corresponding buck converter and outputs a PWM signal of a certain duty ratio for its power MOSFET.

✧ *Control strategy IV：[11];*

In control strategy IV, a distributed MPPT realization with better simplification design is given. The single sensor maximum power tracking strategy was firstly proposed and achieved fast tracking performance with its two-mode operation. This architecture requires only one sensor and the MPPT function is able to be performed for each submodule PV unit through the switch and the common MPPT converter. However, the output of each MPPT converter is connected in parallel which greatly reduces the voltage gain of the system. Moreover, three inductors are still needed. Hence there is opportunity to improve it.

✧ *Control strategy V：[12];*

TABLE I
COMPARATIVE ANALYSIS

		Technique I	Technique II	Technique III	Technique IV	Technique V	Our paper
Components in Power circuit	Inductors	*n*	*n*	*n*	*n*	1	1
	Switches	2n	2n	2n	2n	*2n+2*	2n
	Capacitors	*2n*	*2n*	*2n*	n+1	n+1	n+1
Components in control circuit	Control Units	*n*	1	1	1	1	1
	Sensor and related AD converter	*2n*	n+2	n+1	1	1	1
Other characteristics	Ideal maximum power	Y	*N*	Y	Y	*N*	Y
	Output power ratio	1	1	1	1	*1/N*	1
	Voltage gain	high	high	high	*low*	*low*	high
	Optimal power region	Y	*N*	Y	Y	*N*	Y

Based on single sensor technique in control strategy IV, to further optimize power circuit and reduce system complexity and cost. A multi-channel PV system with single sensor MPPT controller is proposed to track the MPP of each PV unit. The number of components (capacitor, current sensors and voltage sensors and MPPT controller etc.) is decreased in this paper. However, due to the limitation of power circuit, only one PV submodule can output its power at any time during the operation. And two additional switches are needed compared to the other solutions. The requirement for too many converters and high cost is a big issue for further application.

✧ *Our proposal;*

In this paper, three buck stack structure with a common LC filter is applied to against submodule mismatch issue. An OCPT control algorithm is applied accordingly to make fully utilization of one current sensor, one AD unit and one digital controller. The proposal can totally eliminate different small-scaled mismatch effects in real-word condition and the true maximum power point of each PV submodule can be achieved precisely even under rapid irradiance change. For example, comparing with control strategy V, the complexity of power circuit is further optimized in our manuscript, the number of power switches is only 2*N* which is less than that in control strategy V (2*N*+2). The voltage gain of circuit proposed in this paper is three times as high as that in control strategy V, which means another high voltage gain cascading converter is still needed if control strategy V is used in grid-tied power generation. In control strategy V, the circuit only outputs maximum power of connected PV unit while the other disconnected units are totally lost without any power output. The operating state of each PV unit depends on the enable switch (S_{u1}, S_{u2},....,S_{uN}). In our manuscript, all PV units output their individual maximum power in any time regardless of mismatch case.

Based on the above analysis from different perspectives, the pros and cons have been summarized in Table. I. Compared with other solutions, our proposal proposes an optimized submodule level PV system. It can be integrated into junction box of commercial PV module. The proposal can guarantee ideal maximum power generation of each PV unit regardless of mismatch cases with least components in both power circuit and control circuit comparing with other full power processing solutions.

IV. SIMULATION AND TEST RESULTS

Simulation and hardware test results are provided to verify the proposed structure and strategy. Several related parameters are given in TABLE.II.

TABLE II
PARAMETERS OF VERIFICATION OF OCPT BASED PV MODULE

Parameters		Value
PV Submodules	V_{mpp1}, I_{mpp1}, P_{mpp1} (STC)	10V, 2A, 20W
	V_{mpp2}, I_{mpp2}, P_{mpp2} (STC)	12.5V, 2.5A, 31.25W
	V_{mpp3}, I_{mpp3}, P_{mpp3} (STC)	15V, 3A, 45W
Control Unit	f_s	20kHz
	T_{mppt}	0.05s
	T	20ms

A. Simulation results

Simulation performance is shown in Fig. 6, which presents the voltage waveforms of three submodules. During the first one second, submodule 1 is being tracked and it arrives at its MPP voltage. Then in the next second, the MPPT controller tracks submodule 2 and finally makes it operate at its MPP voltage and outputs 31.25W power. In the period (2s, 3s), submodule 3 is being perturbed and reaches its MPP. At this moment, all submodules operate at their respective MPPs and the similar process repeats. Since all submodules have reached their MPPs, there are just slight oscillations around the MPP voltages in the second round of tracking.

The above simulation results effectively prove that with the OCPT control strategy, the proposed integrated structure can make all of its submodules operate at their individual MPPs regardless of mismatch cases.
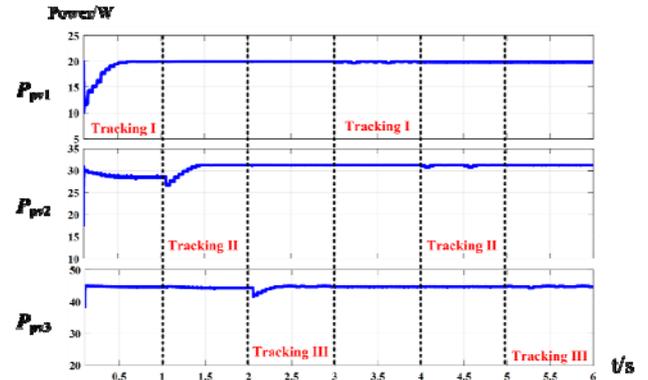

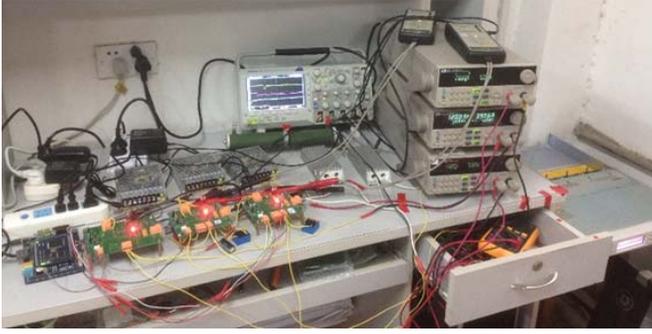Fig. 6. Voltage waveforms of three submodules.

B. Test results

Fig. 7. Testbed.

To further verify the effectiveness of our proposal, the experimental validation of the proposed scheme is carried on and the testbed is shown in Fig.7. A DC voltage source and a series connected power resistor are used to replicate the electrical behavior of a sunlight illuminated PV module in an indoor environment. The output of the proposed structure is connected to an electronic load. Two different cases are tested, as listed in Table III.

TABLE III
PARAMETERS OF OCPT BASED PV MODULE

	Parameters	Value
Test cases	$V_{mpp1}, V_{mpp2}, V_{mpp3}$ (**Case 1**)	10V, 10V,10V
	$V_{mpp1}, V_{mpp2}, V_{mpp3}$ (**Case 2**)	10V, 12.5V,15V
Control Unit	f_s	50kHz
	T_{mppt}	1s
	T	25s

In case 1, all submodules are under the same irradiance case without any mismatch. Fig.8 shows the voltage waveforms of three submodules. (Blue: 1; Purple: 2; Green: 3) In the first 25 seconds, submodule 1 is being tracked, while submodule 2 and 3 are waiting for MPPT. It takes about 8s to reach Vmpp1, 10V and then Vpv1 keeps oscillating around 10V. At 25s, the OCPT controller turns to track MPP for submodule 2 and Vpv2 finally arrives at 10V. During (50s, 75s), the MPPT of submodule 3 is enabled and Vmpp3 is approached. At 75s, all submodules operate at their respective MPPs and there will be just slight oscillations around the MPP voltages in the second round of tracking, as shown in Fig.8.

In case 2, three submodules are under different irradiance cases. Fig.9 shows the voltage waveforms of three submodules of this case. (Blue: 1; Purple: 2; Green: 3) The operating process is similar to case 1, while three submodules reach different MPPs. Submodule 1 is first being tracked, while submodule 2 and 3 are waiting for MPPT. Vpv1 reaches Vmpp1, 10V and keeps oscillating around 10V. During (25s, 50s), the MPPT of submodule 2 is activated and Vmpp2 is approached. At 50s, the OCPT controller turns to perturb the voltage of submodule 3 and Vpv3 finally arrives at 15V. After submodule 3 has achieved its MPPT, all submodules output their respective maximum powers. Unless
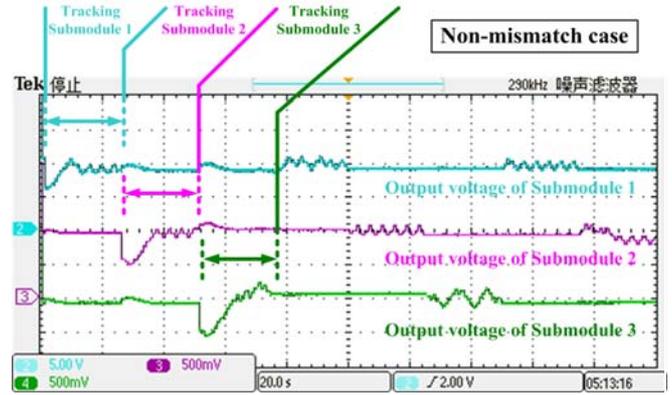

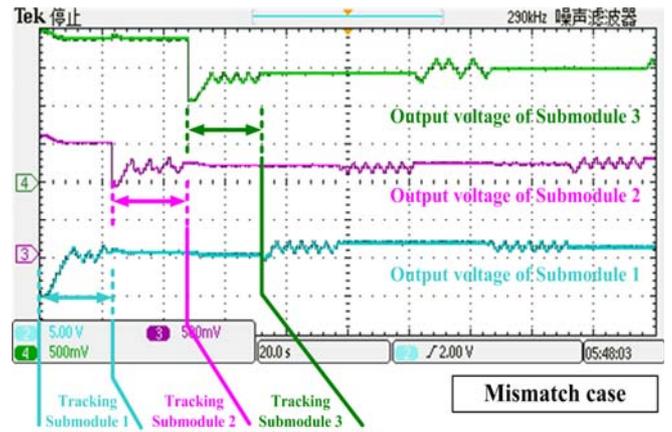Fig. 8. Test result of Case 1.

Fig. 9. Test result of Case 2.

the irradiance changes, there are just slight oscillations around the MPP voltages in the next round of tracking.

Since the output voltages of three submodules are not common ground, we used one ordinary probe (channel 2) to measure the output voltage of submodule I and two differential probes (channel 3 and 4) to respectively measure the output voltages of submodule 2 and 3. The differential probe zooms out the measured voltage and the ratio is 10:1. Therefore the scales of channel 3 and 4 are 500mV. In the experiment case 1, the MPP voltages of three submodules are all 10V, the P-V and I-V curves are shown as blue curves in Fig.10. It can be seen in Fig.8 in manuscript that all submodules reach 10V. Similarly, in case 2, the MPP voltages of three submodules are supposed to be 10V, 12.5V and 15V. It can be seen in Fig.9 that three submodules indeed reach 10V, 12.5V and 15V. Therefore, the MPP tracking
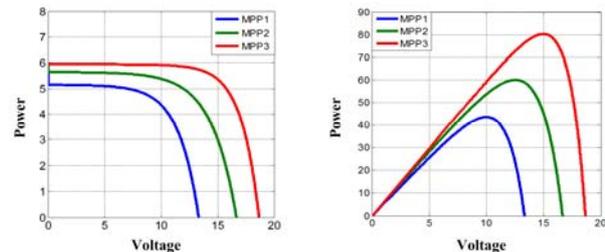

Fig. 10. Testbed.

ability is sufficiently verified.

Obviously, the experimental results validate the effectiveness and viability of our proposed scheme. Using the OCPT control strategy, the submodule level Buck stack structure can precisely track the individual MPPs of all submodules regardless of mismatch cases.

V. CONCLUSIONS

Simplification and optimization have been the direction of development of DMPPT PV system especially in submodule level application. However, there is always a tradeoff between mismatch power loss and exponentially increasing components. This paper proposed a submodule level maximum power generation solution against small scale shading cases in real-world. The proposed integrated submodule level PV structure along with OCPT control strategy can not only eliminate mismatch power loss, but also enjoy the least components comparing with current solutions. Meanwhile, the true MPP of each PV submodule can always be guaranteed even under rapid irradiance changes. The proposed low-cost submodule DMPPT solution and control algorithm provide very promising power savings compared to the conventional MPPT approach. Enormous potential of the proposed system with limited control unit and components can be fully developed to achieve more integrated, modularized, intellectual PV systems in the future.

REFERENCES

[1] S. Qin, C. B. Barth, and R. C. N. Pilawa-Podgurski, "Enhancing Microinverter Energy Capture With Submodule Differential Power Processing," Power Electronics, IEEE Transactions on, vol. 31, pp. 3575-3585, 2016.

[2] K. A. Kim, P. S. Shenoy, and P. T. Krein, "Converter Rating Analysis for Photovoltaic Differential Power Processing Systems," Power Electronics, IEEE Transactions on, vol. 30, pp. 1987-1997, 2015.

[3] Y. T. Jeon, H. Lee, K. A. Kim, and J. h. Park, "Least Power Point Tracking Method for Photovoltaic Differential Power Processing Systems," IEEE Transactions on Power Electronics, vol. PP, pp. 1-1, 2016.

[4] W. Feng, W. Xinke, F. C. Lee, W. Zijian, K. Pengju, and Z. Fang, "Analysis of Unified Output MPPT Control in Subpanel PV Converter System," Power Electronics, IEEE Transactions on, vol. 29, pp. 1275-1284, 2014.

[5] C. Olalla, D. Clement, M. Rodriguez, and D. Maksimovic, "Architectures and Control of Submodule Integrated DC-DC Converters for Photovoltaic Applications," Power Electronics, IEEE Transactions on, vol. 28, pp. 2980-2997, 2013.

[6] O. Khan, X. Weidong, and H. H. Zeineldin, "Gallium-Nitride-Based Submodule Integrated Converters for High-Efficiency Distributed Maximum Power Point Tracking PV Applications," Industrial Electronics, IEEE Transactions on, vol. 63, pp. 966-975, 2016.

[7] R. C. N. Pilawa-Podgurski and D. J. Perreault, "Submodule Integrated Distributed Maximum Power Point Tracking for Solar Photovoltaic Applications," Power Electronics, IEEE Transactions on, vol. 28, pp. 2957-2967, 2013.

[8] C. Zhongsheng, L. Qiang, and F. C. Lee, "Multi-phase smart converter for PV system," in Applied Power Electronics Conference and Exposition (APEC), 2015 IEEE, 2015, pp. 1736-1742.

[9] F. Wang, T. Zhu, F. Zhuo, H. Yi, S. Shi, and X. Zhang, "Analysis and Optimization of Flexible MCPT Strategy in Submodule PV Application," IEEE Transactions on Sustainable Energy, vol. 8, pp. 249-257, 2017.

[10] Q. Shibin, S. T. Cady, A. D. Dominguez-Garcia, and R. C. N. Pilawa-Podgurski, "A Distributed Approach to Maximum Power Point Tracking for Photovoltaic Submodule Differential Power Processing," Power Electronics, IEEE Transactions on, vol. 30, pp. 2024-2040, 2015.

[11] J. A. A. Qahouq and Y. Jiang, "Distributed photovoltaic solar system architecture with single-power inductor single-power converter and single-sensor single maximum power point tracking controller," IET Power Electronics, vol. 7, pp. 2600-2609, 2014.

[12] Y. Jiang and J. A. A. Qahouq, "Single-sensor multi-channel maximum power point tracking controller for photovoltaic solar systems," IET Power Electronics, vol. 5, pp. 1581-1592, 2012.

[13] S. Lyden and M. E. Haque, "A Simulated Annealing Global Maximum Power Point Tracking Approach for PV Modules Under Partial Shading Conditions," IEEE Transactions on Power Electronics, vol. 31, pp. 4171-4181, 2016.

[14] M. Seyedmahmoudian, R. Rahmani, S. Mekhilef, A. Maung Than Oo, A. Stojcevski, T. Soon, et al., "Simulation and Hardware Implementation of New Maximum Power Point Tracking Technique for Partially Shaded PV System Using Hybrid DEPSO Method," Sustainable Energy, IEEE Transactions on, vol. PP, pp. 1-13, 2015.

[15] F. Wang, F. Zhuo, F. C. Lee, T. Zhu, and H. Yi, "Analysis of Existence-Judging Criteria for Optimal Power Regions in DMPPT PV Systems," IEEE Transactions on Energy Conversion, vol. 31, pp. 1433-1441, 2016.

[16] X. Weidong, N. Ozog, and W. G. Dunford, "Topology Study of Photovoltaic Interface for Maximum Power Point Tracking," Industrial Electronics, IEEE Transactions on, vol. 54, pp. 1696-1704, 2007.

[17] D. Shmilovitz, "On the control of photovoltaic maximum power point tracker via output parameters," Electric Power Applications, IEE Proceedings -, vol. 152, pp. 239-248, 2005.

[18] S. Poshtkouhi, J. Varley, R. Popuri, and O. Trescases, "Analysis of distributed peak power tracking in photovoltaic systems," in Power Electronics Conference (IPEC), 2010 International, 2010, pp. 942-947.

[19] L. Xiong, F. Zhuo, F. Wang, X. Liu, Y. Chen, M. Zhu, et al., "Static Synchronous Generator Model: A New Perspective to Investigate Dynamic Characteristics and Stability Issues of Grid-Tied PWM Inverter," IEEE Transactions on Power Electronics, vol. 31, pp. 6264-6280, 2016.
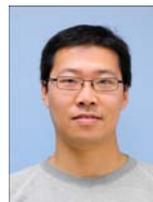
Feng Wang (S'08, M'13) received the B.S., M.S. and Ph.D. degrees in Electrical Engineering from Xi'an Jiaotong University (XJTU), Xi'an China, in 2005, 2009 and 2013, respectively. From November 2010 to November 2012, he was an exchanging Ph.D. student in Center for Power Electronics Systems (CPES) at Virginia Polytechnic Institute and State University, Blacksburg, VA. In November 2013, he joined Xi'an Jiaotong University as a

Postdoctoral Fellow. His current research interests include DC/DC conversion, digital control of switched converters, especially in renewable energy generation fields. F. Wang is with the State Key Laboratory of Electrical Insulation and Power Equipment, School of Electrical Engineering, Xi'an Jiaotong University, Xi'an, Shaanxi 710049, P.R. China (e-mail: fengwangee@xjtu.edu.cn).

Tianhua Zhu (S'16) received the B.S. degree in electrical engineering from Xi'an Jiaotong University (XJTU), Xi'an China, in 2014. She is now pursuing her master's degree in Power Electronics and Renewable Energy Center (PEREC) in Xi'an Jiaotong University (XJTU). Her current research interests include Maximum Power Point Tracking techniques, Distributed Maximum Power Point Tracking and Differential Power Processing. T. Zhu is with the State Key Laboratory of Electrical Insulation and Power Equipment, School of Electrical Engineering, Xi'an Jiaotong University, Xi'an, Shaanxi 710049, P.R. China (e-mail: zth1222@stu.xjtu.edu.cn).

Fang Zhuo (M'00) was born in Shanghai, China, in 1962. He received the B.S. degree in automatic control, and the M.S. and Ph.D. degrees in automation and electrical engineering, respectively, all from Xi'an Jiaotong University, Xi'an, China, in 1984, 1989, and 2001, respectively. He was an Associate Professor at Xi'an Jiaotong University in 1996, and a Full Professor in power electronics and drives in 2004. Then, he worked as a supervisor of Ph.D. students. His research interests include power electronics, power quality, active power filter, reactive power compensation, inverters for distributed power generation, etc. He is the key finisher of four projects sponsored by National Natural Science Foundation of China, and more than 40 projects cooperated with companies from industry. He received four provincial and ministerial level science and technology advancement awards. And four patents are applying or owned by him. He is a member of China Electro Technical Society, Automation Society, and Power Supply Society. He is also the Power Quality Professional Chairman of Power Supply Society in China.
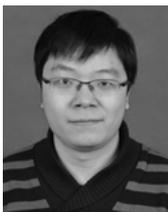
Hao Yi (S'10–M'14) received the M.S. and Ph.D. degrees in electrical engineering from Xi'an Jiaotong University, Xi'an, China, in 2010 and 2013, respectively. Since 2013, he has been a Member of School of Electrical Engineering at Xi'an Jiaotong University. His current research interests include modeling and control of high-power converter, control and power management of microgrid, and power quality improvement.

Shuhuai Shi (S'15) received the B.S. degree in Electrical Engineering from Henan Polytechnic University, Jiaozuo, China, in 2012, and he is currently working toward the Ph.D. degree in the State Key Laboratory of Electrical Insulation and Power Equipment, School of Electrical Engineering, Xi'an Jiaotong University (XJTU), Xi'an, China. His research interests include the topology, control and modulation of the high voltage and high power DC/DC converter, also modeling and control of modular multilevel converter. (e-mail:shishuhuai@stu.xjtu.edu.cn)